



Effect of annealing temperature and cadmium doping on structure and magnetic properties of neodymium orthoferrite nanoparticles synthesized by a simple co-precipitation method

Thi Kim Chung Nguyen¹, Anh Tien Nguyen², Valentina O. Mittova³, Hong Diem Chau², Thi Lan Nguyen⁴, Irina Ya. Mittova⁵, Xuan Vuong Bui^{6,*}

¹Thu Dau Mot University, Thu Dau Mot City, Binh Duong Province, 590000, Vietnam

²Ho Chi Minh City University of Education, Ho Chi Minh City 700000, Vietnam

³Teaching University Geomedi, LLC, 4 King Solomon II str. Tbilisi 0114, Georgia

⁴Advanced Institute for Science and Technology (AIST), Hanoi University of Science and Technology (HUST), Hanoi 10000, Vietnam

⁵Voronezh State University, Voronezh 394018, Russia

⁶Sai Gon University, Ho Chi Minh City 700000, Vietnam

Received 22 March 2022; Received in revised form 23 June 2022; Accepted 26 September 2022

Abstract

A series of $Nd_{1-x}Cd_xFeO_3$ ($x = 0.1, 0.2$ and 0.3) nanoparticles were successfully synthesized from Nd(III), Cd(II) and Fe(III) nitrates by a simple co-precipitation method in boiling water with a 5% sodium hydroxide aqueous solution (without any surfactants) and annealed at 700, 850 and 950 °C for 1 h. SEM and TEM analyses showed particle sizes in the range of 50–70 nm. According to XRD the average crystallite size increased with the annealing temperature, but decreased when the cadmium concentration increased. As the annealing temperature was raised from 700 to 950 °C, the magnetic properties, such as coercivity (H_c), remanent magnetization (M_r) and saturation magnetization (M_s), of the $Nd_{0.8}Cd_{0.2}FeO_3$ sample also increased. In general, the H_c , M_r and M_s values increased with the degree of cadmium doping. The synthesized $Nd_{1-x}Cd_xFeO_3$ nanopowders have much larger coercivity values than some other rare-earth perovskites, such as $Nd_{1-x}Sr_xFeO_3$, $NdFe_{1-x}Co_xO_3$, $LaFe_{1-x}Ti_xO_3$, $YFe_{1-x}Ni_xO_3$, $Y_{1-x}Cd_xFeO_3$, $La_{1-x}Cd_xFeO_3$ or $Bi_{1-x}Cd_xFeO_3$. The high H_c value (1916.52–4833.41 Oe) of the synthesized $Nd_{1-x}Cd_xFeO_3$ nanopowders enables their use for permanent magnets or magnetic recording on hard disks and tapes.

Keywords: nanoparticles, orthoferrite, neodymium, Cd-doping, magnetic properties

I. Introduction

Nano-sized $LnFeO_3$ rare-earth orthoferrites (in which Ln is 4f rare-earth element, such as Ho, Pr, Nd, La, Y, Sm, Eu, etc.) have been studied and applied in many fields, such as catalysis, electrodes for Li-ion batteries, gas-sensors, electro-optical and electromagnetic devices [1–5]. The structural parameters and properties of rare-earth orthoferrites depend on various factors, such as the crystal size, the particle size and morphology, the nature of doping elements, the degree of doping and

also the synthesis method [6–10]. Amongst the most interesting rare-earth orthoferrites, $NdFeO_3$ has attracted much attention. Previously, neodymium orthoferrite had been studied for applications such as As^{5+} adsorption in aqueous solutions [11]. Their structure, optical properties, magnetic properties, and electrical properties have also been analysed [12–14]. In the work of Anand *et al.* [15], the doping of La, Pr and Sm significantly affected the optical absorbance and band gap energy value of $NdFeO_3$ nanomaterials synthesized by the citric acid sol-gel method. The obtained $Nd_{0.5}Ln_{0.5}FeO_3$ (Ln = La, Pr, Sm) nanomaterials had strong absorption both in the UV and Vis regions [15]. The calculated band gap energy (E_g) values were 3.70, 3.80 and 3.76 eV for the

*Corresponding author: tel: +84 816517788
e-mail: bxvuong@sgu.edu.vn

NdFeO₃ doped with La, Pr and Sm, respectively, while the pure NdFeO₃ had E_g of 4.3 eV [16]. The shift of the absorbance of the material from the UV region to the Vis region along with the reduction of band gap energy gives the La, Pr and Sm-doped NdFeO₃ materials great potential in the application as photocatalysts under sunlight [17,18].

Doped NdFeO₃ orthoferrite materials have been synthesized by several methods, such as solid state reaction [13,14,16,19], microwave assisted [21], hydrothermal [2,22,23], co-precipitation using surfactants [24], and sol-gel or gel combustion with the addition of various polymers [15,25,26]. In previous studies [27–31], the authors successfully synthesized LnFeO₃ nanoparticles (Ln = Y, Nd, Pr, Ho) with several doping elements, such as Sr, Co, Ca and Ni by simple co-precipitation via the hydrolysis of cations in hot water ($\geq 95^\circ\text{C}$) and precipitation at room temperature (without any surfactant). Cd is also a divalent metal with an ionic radius of 0.097 nm, which is comparable to that of Ca²⁺ (0.104 nm) and Nd³⁺ (0.094 nm) [32]. Previous studies of Cd-doped LnFeO₃ (Ln = La, Y) showed an increment in the saturation magnetization and coercivity similar to that of Ca-doped LnFeO₃ [33–37]. However, there has been no publication on the influence of cadmium doping on the structural and magnetic properties of NdFeO₃ nanoparticles synthesized by the aforementioned co-precipitation method. The importance of rare earth orthoferrites in many applications prompted us to investigate the effects of annealing temperature and Cd²⁺ doping on the structure and magnetic properties of NdFeO₃ orthoferrite nanomaterials.

Therefore, the objective of this work was to study the effect of annealing temperature and cadmium doping on the structure and magnetic properties of NdFeO₃ orthoferrite nanoparticles synthesized by a simple co-precipitation (without any surfactant).

II. Experimental

The starting materials for preparation of the Nd_{1-x}Cd_xFeO₃ nanoparticles included Nd(NO₃)₃·6H₂O (99.8% purity, Merck), Cd(NO₃)₂·4H₂O (99.7% purity, Sigma-Aldrich), Fe(NO₃)₃·9H₂O (99.6% purity, Sigma-Aldrich) and NaOH (99.7% purity, Sigma-Aldrich), which were used directly without further purification.

Nd_{1-x}Cd_xFeO₃ orthoferrite nanoparticles ($x = 0.1, 0.2$ and 0.3) were synthesized by a co-precipitation method based on the technique previously used for preparation of Nd_{1-x}Sr_xFeO₃ nanoparticles [28]. The difference was that the precipitating agent 5% (NH₄)₂CO₃ was replaced by NaOH 5% solution. A solution (50 ml) containing mixture of Nd(NO₃)₃·6H₂O, Cd(NO₃)₂·4H₂O and Fe(NO₃)₃·9H₂O with suitable molar ratio was added very slowly to 400 ml of boiling water ($\geq 95^\circ\text{C}$) and homogenised on a magnetic stirrer. After mixing, a reddish-brown colour system was obtained. As demon-

strated in the earlier works on the synthesis of LaFeO₃ and YFeO₃ nano orthoferrites [38,39], by slowly adding the mixture of Nd(III), Cd(II) and Fe(III) salts in water at high temperature, the hydrolysis of metal cations could be accelerated, which limited the increase in the particle size of the obtained Nd_{1-x}Cd_xFeO₃ orthoferrites. Next, a NaOH 5% solution was slowly added to the above obtained system until the pH = 9.0 [29]. The formed precipitate was stirred for 45 min, vacuum filtered and washed several times with distilled water until the filtrate had a pH of ~ 7.0 [28]. The precipitate was dried at 105°C for 3 h to remove moisture and then finely ground with a mortar and pestle to obtain a yellowish-brown powder (Nd_{1-x}Cd_xFeO₃ precursor powders). The Nd_{0.8}Cd_{0.2}FeO₃ precursor was annealed at 700, 850 and 950 °C for 1 h to study the formation of the single-phase orthorhombic Nd_{0.8}Cd_{0.2}FeO₃ nanoparticles and the effect of temperature on their properties. From these results, an appropriate annealing temperature for other two Nd_{1-x}Cd_xFeO₃ ($x = 0.1$ and 0.3) powders were determined and the influence of Cd-doping on structure and magnetic properties of the NdFeO₃ orthoferrite nanoparticles was investigated.

Powder X-ray diffraction analysis (PXRD) of the obtained Nd_{1-x}Cd_xFeO₃ samples was carried out using a D8-Advance X-ray diffractometer (Germany) with CuK _{α} radiation ($\lambda = 0.154184$ nm, angle range of $2\theta = 10\text{--}80^\circ$, scan rate of $0.02^\circ/\text{s}$). The average crystallite size (D) of the Nd_{1-x}Cd_xFeO₃ samples was calculated by the Debye-Scherrer formula. Morphology and particle size of the obtained Nd_{1-x}Cd_xFeO₃ samples were determined by transmission electron microscopy (TEM, JEOL JEM-1400, Japan) and scanning electron microscopy (FE-SEM, S-4800, Japan).

The hysteresis loop and magnetic properties, including the coercivity (H_c), remanent magnetization (M_r) and saturation magnetization (M_s) were recorded on a vibrating sample magnetometer (VSM, MICROSENE EV11) under the maximal magnetic field of ± 20 kOe.

III. Results and discussion

Figure 1a shows PXRD patterns of the Nd_{0.8}Cd_{0.2}FeO₃ sample annealed at 700, 850 and 950 °C. The results showed that all three samples exhibited peaks matching with the standard orthorhombic NdFeO₃, *Pbnm* (62) space group (JCPDS No. 74-1473) [28]. No peaks of impurities, such as Nd₂O₃, Fe₂O₃, Fe₃O₄, CdO or CdFe₂O₄ were observed, proving the successful doping of cadmium into the orthorhombic NdFeO₃ crystal lattice. When the annealing temperature was raised from 700 to 850 °C, the degree of crystallinity of the Nd_{0.8}Cd_{0.2}FeO₃ sample increased significantly and then decreased slightly when the sample was annealed at 950 °C. In addition, when the annealing temperature increased, the average crystal size also increased, i.e. $D_{700^\circ\text{C}} = 29.4$ nm, $D_{850^\circ\text{C}} = 35.7$ nm and $D_{950^\circ\text{C}} = 53.1$ nm (Table 1).

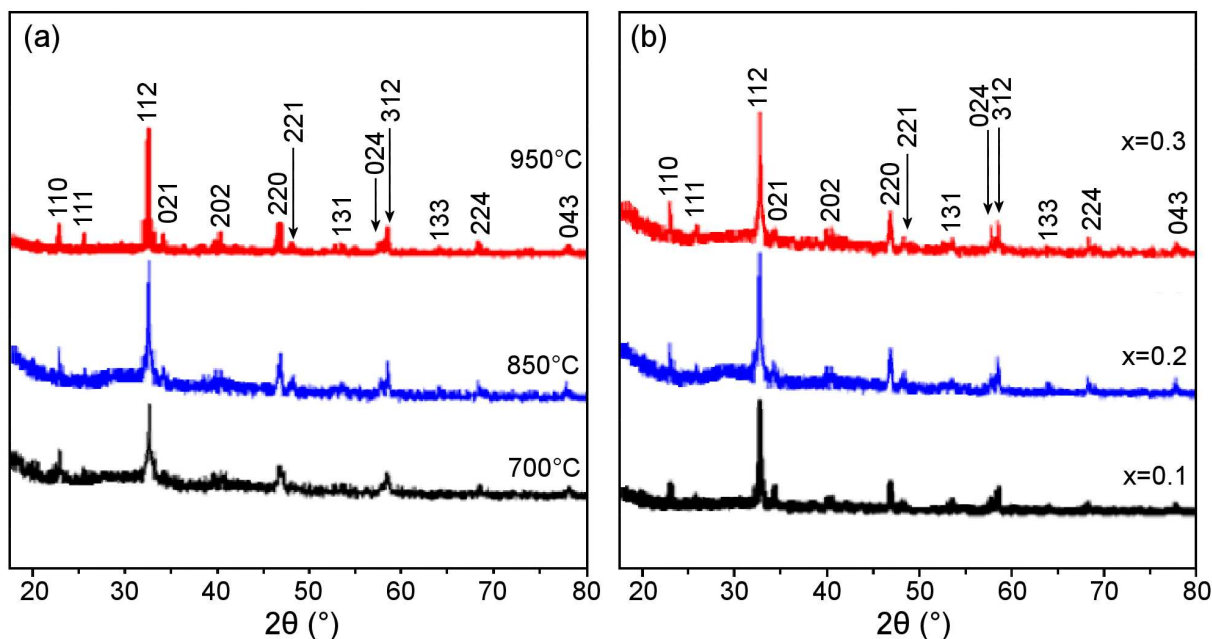


Figure 1. PXRD patterns of $\text{Nd}_{0.8}\text{Cd}_{0.2}\text{FeO}_3$ annealed at 700, 850 and 950 °C (a) and of $\text{Nd}_{1-x}\text{Cd}_x\text{FeO}_3$ annealed at 850 °C (b)

Table 1. Structural parameters of $\text{Nd}_{1-x}\text{Cd}_x\text{FeO}_3$ nanocrystals synthesized by the co-precipitation method

Samples	$2\theta_{112}$ [°]	Height [cts]	d -spacing [Å]	D [nm]
NdFeO_3 , 850 °C [28]	32.5078	197.52	2.74585	29.8
$\text{Nd}_{0.8}\text{Cd}_{0.2}\text{FeO}_3$, 700 °C	32.6357	84.48	2.74301	29.4
$\text{Nd}_{0.8}\text{Cd}_{0.2}\text{FeO}_3$, 850 °C	32.6232	211.18	2.74708	35.7
$\text{Nd}_{0.8}\text{Cd}_{0.2}\text{FeO}_3$, 950 °C	32.6179	203.60	2.74956	53.1
$\text{Nd}_{0.9}\text{Cd}_{0.1}\text{FeO}_3$, 850 °C	32.6102	185.20	2.74226	42.5
$\text{Nd}_{0.7}\text{Cd}_{0.3}\text{FeO}_3$, 850 °C	32.6328	223.65	2.73973	34.1

Table 1 shows that the crystallinity values of the $\text{Nd}_{0.8}\text{Cd}_{0.2}\text{FeO}_3$ samples, annealed at 700 and 850 °C, are approximately the same, while the crystallite size of the sample annealed at 850 °C is much smaller than that of the sample annealed at 950 °C. Therefore, temperature of 850 °C was chosen to anneal the $\text{Nd}_{0.9}\text{Cd}_{0.1}\text{FeO}_3$ and $\text{Nd}_{0.7}\text{Cd}_{0.3}\text{FeO}_3$ precursors to study the effect of Cd-content on structure and magnetic properties of the $\text{Nd}_{1-x}\text{Cd}_x\text{FeO}_3$ nanoparticles.

Figure 1b depicts PXRD patterns of the $\text{Nd}_{1-x}\text{Cd}_x\text{FeO}_3$ samples ($x = 0.1, 0.2$ and 0.3) annealed at 850 °C for 1 h. XRD peaks of all three $\text{Nd}_{1-x}\text{Cd}_x\text{FeO}_3$ samples with $x = 0.1, 0.2$ and 0.3 appear at the same positions as those of the standard NdFeO_3 (JCPDS No. 74-1473) with no observable impurity peaks. Hence, all $\text{Nd}_{1-x}\text{Cd}_x\text{FeO}_3$ samples are single-phase perovskites with an orthorhombic structure, $Pnma$ (62) space group. As the concentration of Cd-doping increased from 0.1 to 0.3, the 2θ diffraction angle for the peak with the highest intensity (corresponding to (112) plane) also increased, shifting 2θ angle to the right (Fig. 2 and Table 1). It can be explained with the fact that the Cd^{2+} ionic radius ($r = 0.097$ nm) is larger than that of Nd^{3+} ($r = 0.094$ nm) [32]. Similar results were reported by Vo *et al.* [28] for $\text{Nd}_{1-x}\text{Sr}_x\text{FeO}_3$ perovskite (ionic radius

of Sr^{2+} is 0.112 nm) and by Berezhnaya *et al.* [8] for $\text{La}_{1-x}\text{Ba}_x\text{FeO}_3$ perovskite where ionic radius of Ba^{2+} ($r = 0.134$ nm) is larger than that of La^{3+} ($r = 0.104$ nm). However, with the increase of x , the full width at half maximum (FWHM) tended to widen, meaning a decrease in the crystallite size (Table 1). When Cd^{2+} is doped into the $\text{Nd}^{\text{III}}\text{Fe}^{\text{III}}\text{O}_3$ crystal lattice, part of the

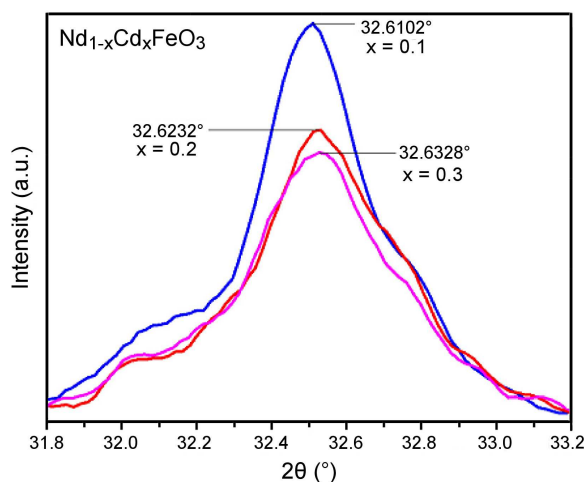
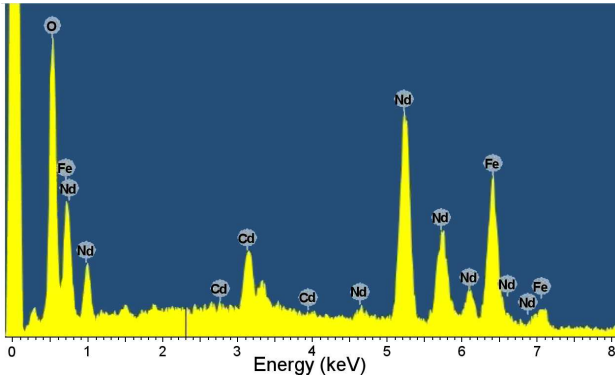


Figure 2. The magnified XRD patterns of peaks at $2\theta \sim 32.4\text{--}32.8^\circ$

Table 2. EDX analysis of $\text{Nd}_{1-x}\text{Cd}_x\text{FeO}_3$ nanosized powders annealed at 850 °C

Nominal formulas	Nd [at.%]	Cd [at.%]	Fe [at.%]	O [at.%]	Real formulas
$\text{Nd}_{0.9}\text{Cd}_{0.1}\text{FeO}_3$	16.90	1.86	19.20	62.04	$\text{Nd}_{0.88}\text{Cd}_{0.097}\text{FeO}_{3.23}$
$\text{Nd}_{0.8}\text{Cd}_{0.2}\text{FeO}_3$	14.18	3.27	18.18	64.37	$\text{Nd}_{0.78}\text{Cd}_{0.18}\text{FeO}_{3.54}$
$\text{Nd}_{0.7}\text{Cd}_{0.3}\text{FeO}_3$	11.73	4.55	17.51	66.21	$\text{Nd}_{0.67}\text{Cd}_{0.26}\text{FeO}_{3.78}$

**Figure 3.** EDX analysis of $\text{Nd}_{0.8}\text{Cd}_{0.2}\text{FeO}_3$ sample annealed at 850 °C for 1 h

Fe^{3+} ions could be oxidized to Fe^{4+} ions to balance the local charge ($\text{Fe}^{3+} \rightarrow \text{Fe}^{4+} + e^-$, and $r_{\text{Fe}^{4+}} < r_{\text{Fe}^{3+}}$), leading to an increase in Fe^{4+} ion concentration and internal stress with the degree of Cd-doping, and finally resulting in the decrease in crystallite size according to Vegard's law [40,41]. The increase in Fe^{4+} content with increasing x is also consistent with the EDX results and the observed increase in oxygen content (Fig. 3 and Table 2).

Elemental composition analysis from EDX shows that no impurity element apart from Nd, Cd, Fe and O was detected in the $\text{Nd}_{1-x}\text{Cd}_x\text{FeO}_3$ nanomaterials (Fig. 3). The atom percentage of each element is also in accordance with their ratio in the nominal formulas (Table 2). As the solubility product constants of corresponding hydroxides are very small ($1.10 \cdot 10^{-21}$ for $\text{Nd}(\text{OH})_3$, $2.39 \cdot 10^{-14}$ for $\text{Cd}(\text{OH})_2$, and $2.79 \cdot 10^{-39}$ for $\text{Fe}(\text{OH})_3$) [32], Nd^{3+} , Cd^{2+} and Fe^{3+} ions easily precipitated with

OH^- [32]. The increase in the percentage of oxygen atoms when x increased from 0.1 to 0.3, as explained above, was due to a part of Fe^{3+} ions being oxidized to Fe^{4+} ions [28,39–41]. Similar results were observed for some other rare earth perovskites, such as $\text{Nd}_{1-x}\text{Sr}_x\text{FeO}_3$ [28], $\text{La}_{1-x}\text{Ba}_x\text{FeO}_3$ [8] and $\text{Y}_{1-x}\text{Ba}_x\text{FeO}_3$ [10].

In previous reports [28,30,31,36], SEM and TEM studies did not prove a significant effect of different doping elements on the particle size of LnFeO_3 ($\text{Ln} = \text{La}, \text{Y}, \text{Ho}, \text{Nd}$) powders. Therefore, here we presented SEM and TEM images only of the $\text{Nd}_{0.8}\text{Cd}_{0.2}\text{FeO}_3$ sample annealed at 850 °C for 1 h (Fig. 4). The annealed $\text{Nd}_{0.8}\text{Cd}_{0.2}\text{FeO}_3$ sample shows a quite uniform particle morphology and size: the particles are almost spherical with a size of 50–70 nm. However, difficulties in the dispersion of the particles due to their magnetic attraction resulted in aggregation and stacked clusters. Particle agglomeration was also observed for similar perovskites such as $\text{Nd}_{1-x}\text{Sr}_x\text{FeO}_3$, $\text{LaFe}_{1-x}\text{Ni}_x\text{O}_3$ or $\text{NdFe}_{1-x}\text{Co}_x\text{O}_3$ [28,30,31].

The magnetic studies at room temperature (Figs. 5 and 6) showed that the annealing temperature and the degree of Cd-doping content affected not only the structural, but also the magnetic properties of the $\text{Nd}_{1-x}\text{Cd}_x\text{FeO}_3$ nanoparticles ($x = 0.1, 0.2$ and 0.3). Indeed, all three magnetic values (H_c , M_r and M_s) increased with annealing temperature for the $\text{Nd}_{0.8}\text{Cd}_{0.2}\text{FeO}_3$ nanopowder (except for the sample annealed at 850 °C, which had the lowest M_s). H_c and M_r values increased due to an increase in crystallite size when the annealing temperature was raised from 700 to 950 °C. Nanoparticles ($D < 100$ nm) can be considered as single-domain particles and then the coercivity

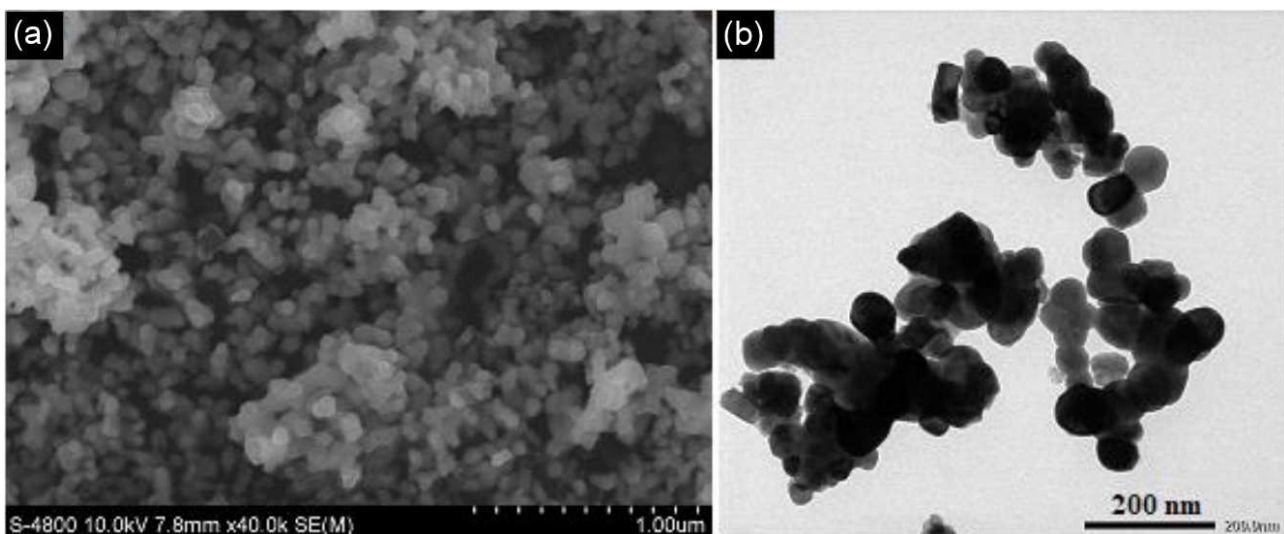
**Figure 4.** SEM (a) and TEM (b) images of the $\text{Nd}_{0.8}\text{Cd}_{0.2}\text{FeO}_3$ sample annealed at 850 °C for 1 h

Table 3. Magnetic properties of Nd_{1-x}Cd_xFeO₃ nanopowders at 300 K

Samples	H _c [Oe]	M _r [emu/g]	M _s [emu/g]
NdFeO ₃ , 850 °C [28]	62.27	0.0031	0.15
Nd _{0.8} Cd _{0.2} FeO ₃ , 700 °C	1916.52	0.14	0.97
Nd _{0.8} Cd _{0.2} FeO ₃ , 850 °C	3747.05	0.17	0.82
Nd _{0.8} Cd _{0.2} FeO ₃ , 950 °C	4833.41	0.24	1.02
Nd _{0.9} Cd _{0.1} FeO ₃ , 850 °C	3753.04	0.20	0.95
Nd _{0.7} Cd _{0.3} FeO ₃ , 850 °C	4250.05	0.21	0.93

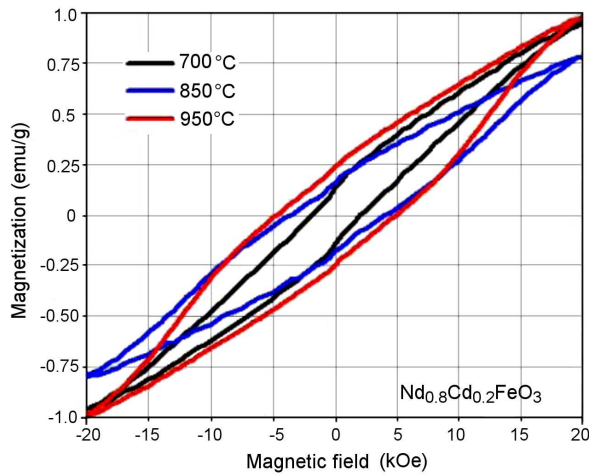


Figure 5. Room-temperature magnetic hysteresis loops of Nd_{0.8}Cd_{0.2}FeO₃ nanoparticles annealed at 700, 850 and 950 °C for 1 h

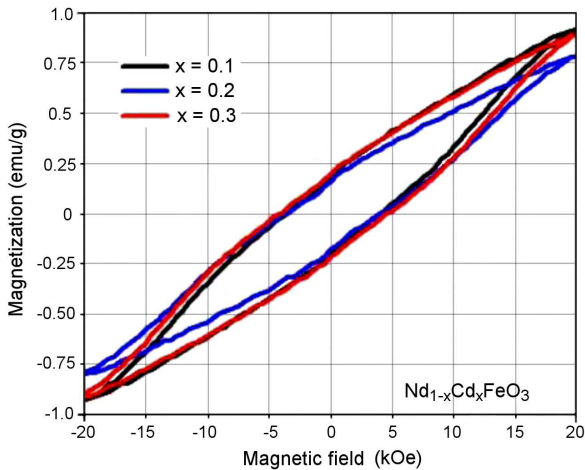


Figure 6. Room-temperature magnetic hysteresis loops of Nd_{1-x}Cd_xFeO₃ nanoparticles annealed at 850 °C for 1 h

depends on the particle size according to the following formula [42]:

$$H_c = g - \frac{h}{D^{3/2}} \quad (1)$$

where *g* and *h* are constants, *D* is the particle size. Accordingly, *H_c* will increase as the particle size of the sample increases. Indeed, for the sample Nd_{0.8}Cd_{0.2}FeO₃, when the annealing temperature increased from 700 to 950 °C, the crystallite size increased from 29.4 to 53.1 nm (Table 1) and *H_c* also

increased from 1916.5 Oe to 4833.4 Oe (Table 3). Although the crystallite size of the Nd_{1-x}Cd_xFeO₃ decreased with the increment of Cd²⁺ ions concentration in the NdFeO₃ crystal lattice (Table 1), the *H_c* value of the Nd_{0.7}Cd_{0.3}FeO₃ (*H_c* = 4250.0 Oe) was much higher than that of the Nd_{0.9}Cd_{0.1}FeO₃ (*H_c* = 3753.0 Oe) and Nd_{0.8}Cd_{0.2}FeO₃ (*H_c* = 3747.0 Oe). This can be explained by the increase in the magnetic anisotropy in NdFeO₃ as the Cd²⁺ content increased [43]. The exception for the Nd_{0.8}Cd_{0.2}FeO₃ sample annealed at 850 °C (*H_c* and *M_r* values are the lowest) was because of its highest crystallinity (Table 1), meaning a higher crystal stability and lower crystal anisotropy [43]. The anomaly for doping content *x* = 0.2 also occurred for other rare earth perovskites such as La_{1-x}Ba_xFeO₃ [8], LaFe_{1-x}Ti_xO₃ [9], Nd_{1-x}Sr_xFeO₃ [28], YFe_{1-x}Ni_xO₃ [31] or LaFe_{1-x}Ni_xO₃ [44].

The Cd-doped NdFeO₃ orthoferrite nanoparticles prepared in this study have higher coercivity values than those of NdFeO₃ doped with different elements, such as Nd_{1-x}Sr_xFeO₃ [28] or NdFe_{1-x}CoxO₃ [30], and also higher than some other rare earth perovskite systems such as LaFe_{1-x}Ti_xO₃ [9], YFe_{1-x}Ni_xO₃ [31], Y_{1-x}Cd_xFeO₃ [35], La_{1-x}Cd_xFeO₃ [36] or Bi_{1-x}Cd_xFeO₃ [45]. In addition, at the magnetic field *H* = ±20 kOe, the magnetization curve of the Nd_{1-x}Cd_xFeO₃ nanoparticles continued to rise without any sign of saturation. With high coercivity and unsaturated magnetization curve at magnetic field *H* = ±20 kOe, Cd-doped NdFeO₃ nanoparticles can be applied as hard magnetic materials for permanent magnets and magnetic recording in hard drives and magnetic tapes [42].

IV. Conclusions

Cd-doped NdFeO₃ (Nd_{1-x}Cd_xFeO₃ where *x* = 0.1, 0.2 and 0.3) nanoparticles were successfully synthesized by the simple co-precipitation method (without any surfactant) and annealed at different temperatures (700, 850 and 950 °C) for 1 h. The average crystallite size varied between 29.4 and 53.1 nm. The SEM and TEM images show particles with a size of 50–70 nm. In general, the magnetic values increased with the annealing temperature and with the degree of Cd-doping. With a very high coercivity (*H_c* = 1916.5–4833.4 Oe), the synthesized Cd-doped NdFeO₃ nanoparticles can be applied as permanent magnets or magnetic recording materials in hard drives.

References

- A.T. Nguyen, W.G. Kidanu, V.O. Mittova, V.H. Nguyen, D.Q. Nguyen, M.P. Le Loan, I.Ya. Mittova, T. Kim II, T.L. Nguyen, "Tailored HoFeO₃-Ho₂O₃ hybrid perovskite nanocomposite as stable anode material for advanced lithium-ion storage", *Int. J. Energy Res.*, **46** [2] (2021) 2051–2063.
- Z. Zhou, L. Guo, H. Yang, Q. Liu, F. Ye, "Hydrothermal synthesis and magnetic properties of multiferroic rare-earth orthoferrites", *J. Alloys Compd.*, **583** (2014) 21–31.
- A.T. Nguyen, N.T. Nguyen, I.Ya. Mittova, N.S. Perov, V.O. Mittova, T.C.C. Hoang, V.M. Nguyen, V.H. Nguyen, V. Pham, X.V. Bui, "Crystal structure, optical and magnetic properties of PrFeO₃ nanoparticles prepared by modified co-precipitation method", *Proc. Appl. Ceram.*, **14** (2020) 355–361.
- Z.Q. Wang, Y.S. Lan, Z.Y. Zeng, X.R. Chen, Q.F. Chen "Magnetic structures and optical properties of rare-earth orthoferrites RFeO₃ (R = Ho, Er, Tm and Lu)", *Solid State Comm.*, **288** (2019) 10–17.
- T.N. Anh, D.P. Viet, V.O. Mittova, D.N. Hai, N.V. Thuan, L.T. My Linh, H.N. Van, I.Ya. Mittova, M.P. Loan, N.A. Yong, T. Kim II, T.L. Nguyen, "Fabricating nanostructured HoFeO₃ perovskite for lithium-ion battery anodes via co-precipitation", *Scripta Mater.*, **207** (2022) 114259.
- A.T. Nguyen, T.T.L. Nguyen, X.V. Bui, "Influence of the synthetic conditions on the crystal structure, magnetic and optical properties of holmium orthoferrite nanoparticles", *J. Mater. Sci. Mater. Electr.*, **32** (2021) 19010–19019.
- T.K.C. Nguyen, T.N. Anh, X.V. Bui, "Optical and magnetic properties of YFeO₃ nanoparticles synthesized by a co-precipitation method at high temperature", *Chem. Papers*, **76** (2022) 923–930.
- M. V. Berezhnaya, N.S. Perov, O.V. Almjashaeva, V.O. Mittova, T.N. Anh, I.Ya. Mittova, L.V. Druzhinina, Yu.A. Alechina, "Synthesis and magnetic properties of barium-doped nanocrystal lanthanum orthoferrite", *Russ. J. Gen. Chem.*, **89** [3] (2019) 480–485.
- C. Sasikala, N. Durairaj, I. Baskaran, B. Sathyaseelan, M. Henini, "Transition metal titanium (Ti) doped LaFeO₃ nanoparticles for enhanced optical structure and magnetic properties", *J. Alloys Compd.*, **712** (2017) 870–877.
- M.V. Berezhnaya, O.V. Al'myashaeva, V.O. Mittova, T.N. Anh, I.Ya. Mittova, "Sol-gel synthesis and properties of Y_{1-x}Ba_xFeO₃ nanocrystals", *Russ. J. Gen. Chem.*, **88** [4] (2018) 626–631.
- M.D. Luu, N.N. Dao, D.V. Nguyen, N.C. Pham, T.N. Vu, T.D. Doan, "A new perovskite-type NdFeO₃ adsorbent: synthesis, characterization, and As(V) adsorption", *Adv. Natur. Sci. Nanosci. Nanotechn.*, **7** (2016) 025015.
- T.H.D. Pham, T.N. Anh, "Optical and magnetic properties of orthoferrite NdFeO₃ nanomaterials synthesized by simple co-precipitation method", *Cond. Matt. Interp.*, **23** [4] (2021) 600–606.
- V. Zharvan, Y.N. Kamaruddin, S. Samnur, E.H. Sujiono, "The effect of molar ratio on crystal structure and morphology of Nd_{1+x}FeO₃ (x = 0.1, 0.2 and 0.3) oxide alloy material synthesized by solid state reaction method", *IOP Conf. Series Mater. Sci. Eng.*, **202** (2017) 012072.
- P.V. Serna, C.G. Campos, F.S.D. Jesus, A.M.B. Miro, J.A.J. Loran, J. Longwell, "Mechanosynthesis, crystal structure and magnetic characterization of neodymium orthoferrite", *Mater. Res.*, **19** [2] (2016) 0214.
- S. Anand, H. Shahid, M. Samiya, Z. Naima, K. Wasi, "Structure of nanocrystalline Nd_{0.5}R_{0.5}FeO₃ (R = La, Pr, and Sm) intercorrelated with optical, magnetic and thermal properties", *J. Alloys Compd.*, **806** (2019) 1250–1259.
- A.M. Sajad, M. Ikram, K. Asokan, "Effect of Ni doping on optical, electrical and magnetic properties of Nd orthoferrite", *J. Phys. Conf. Series*, **534** (2014) 012017.
- A.N. Tien, T.T.L. Nguyen, X.B. Vuong, H.T.N. Duyen, D.L. Han, M.T.L. Linh, P. Vinh, "Optical and magnetic properties of HoFeO₃ nanocrystals prepared by a simple co-precipitation method using ethanol", *J. Alloys Compd.*, **834** (2020) 155098.
- A.S. Seroglazova, M.I. Chebanenko, V.I. Popkov, "Synthesis, structure and photo-fenton activity of PrFeO₃-TiO₂ mesoporous nanocomposites", *Cond. Matt. Interp.*, **23** [4] (2021) 543–547.
- I. Ahmad, M.J. Akhtar, M. Siddique, "Effect of Ni doping on the structural properties and collapse of magnetic ordering in NdFe_{1-x}Ni_xO₃ (0.1 ≤ x ≤ 0.7) orthoferrites", *Chinese Phys. B*, **25** [2] (2016) 028101.
- I. Ahmad, M.J. Akhtar, M. Siddique, M. Iqbal, M.M. Hasan, "Origin of anomalous octahedral distortions and collapse of magnetic ordering in Nd_{1-x}Sr_xFeO₃ (0 ≤ x ≤ 0.5)", *Ceram. Int.*, **39** [8] (2013) 8901–8909.
- Y. Mostafa, S.Z. Samaneh, K.M. Mozghan, "Synthesis and characterization of nano-structured perovskite type neodymium orthoferrite NdFeO₃", *Current Chem. Lett.*, **6** [1] (2017) 23–30.
- K.O. Ogunniran, G. Murugadoss, R. Thangamuthu, P. Periasamy, "Evaluation of nanostructured Nd_{0.7}Co_{0.3}FeO₃ perovskite obtained via hydrothermal method as anode materials for Li-ion battery", *Mater. Chem. Phys.*, **248** (2020) 122944.
- Y. Wang, X. Yan, J. Chen, J. Deng, R. Yu, X. Xing, "Shape controllable synthesis of NdFeO₃ micro single crystals by a hydrothermal route", *CrystEngComm*, **16** [5] (2014) 858–862.
- M. Khorasani-Motlagh, M. Noroozifar, M. Yousefi, Sh. Jahani, "Chemical synthesis and characterization of perovskite NdFeO₃ nanocrystals via a co-precipitation method", *Int. J. Nanosci. Nanotechn.*, **9** [1] (2013) 7–14.
- O. Opuchovic, G. Kreiza, J. Senvaitiene, K. Kazlauskas, A. Beganskiene, A. Kareiva, "Sol-gel synthesis, characterization and application of selected sub-microsized lanthanide (Ce, Pr, Nd, Tb) ferrites", *Dyes Pigments*, **118** (2015) 176–182.
- E. Tugova, S. Yastrebov, O. Karpov, R. Smith R, "NdFeO₃ nanocrystals under glycine nitrate combustion formation", *J. Cryst. Growth*, **467** (2017) 88–92.
- X.V. Bui, A.T. Nguyen, "Sol-gel synthesis, crystal structure and magnetic properties of nanocrystalline praseodymium orthoferrite", *Cond. Matt. Interp.*, **23** [2] (2021) 196–203.
- Q.M. Vo, V.O. Mittova, V.H. Nguyen, I.Ya. Mittova, A.T. Nguyen, "Strontium doping as a means of influencing the characteristics of neodymium orthoferrite nanocrystals synthesized by co-precipitation method", *J. Mater. Sci. Mater. Electr.*, **32** (2021) 26944–26954.
- A.T. Nguyen, C.H. Truong, X.V. Bui, "Synthesis of holmium orthoferrite nanoparticles by the co-precipitation method at high temperature", *Metal. Mater. Eng.*, **27** [3] (2021) 321–329.
- A.T. Nguyen, L.T. Pham, I.Ya. Mittova, V.O. Mittova,

- T.T.L. Nguyen, V.H. Nguyen, X.V. Bui, “Co-doped NdFeO₃ nanoparticles: Synthesis, optical and magnetic properties study”, *Nanomaterials*, **11** (2021) 937.
31. A.T. Nguyen, V. Pham, H.D. Chau, V.O. Mittova, I.Ya. Mittova, E.L. Kopeychenko, T.T.L. Nguyen, X.V. Bui, T.P.A. Nguyen, “Effect of Ni substitution on phase transition, crystal structure and magnetic properties of nanostructured YFeO₃ perovskite”, *J. Molec. Struct.*, **1215** (2020) 128293.
 32. J.E. House, *Inorganic Chemistry*, 2nd Ed., Academic Press, Elsevier, 2012.
 33. A.T. Nguyen, I.Ya. Mittova, D.O. Solodukhin, O.V. Al'myasheva, V.O. Mittova, S.Yu. Demidova, “Sol-gel formation and properties of nanocrystals of solid solution Y_{1-x}Ca_xFeO₃”, *Russ. J. Inorg. Chem.*, **59** [2] (2014) 40–45.
 34. M.B. Bellakki, V. Manivannan, J. Das, “Synthesis, structural and magnetic properties of La_{1-x}Cd_xFeO₃ (0.0 ≤ x ≤ 0.3) orthoferrites”, *Mater. Res. Bull.*, **44** [7] (2009) 1522–1527.
 35. V.T. Dinh, V.O. Mittova, O.V. Almjasheva, I.Ya. Mittova, “Synthesis and magnetic properties of nanocrystalline Y_{1-x}Cd_xFeO_{3-δ} (0 ≤ x ≤ 0.2)”, *Inorg. Mater.*, **47** [10] (2011) 1141–1146.
 36. E.I. Kopeychenko, I.Ya. Mittova, N.S. Perov, A.T. Nguyen, V.O. Mittova, Yu.A. Alekhina, V. Pham, “Synthesis, composition and magnetic properties of cadmium-doped lanthanum ferrite nanopowders”, *Inorg. Mater.*, **57** [4] (2021) 367–371.
 37. F. Bidrawn, S. Lee, J.M. Vohs, R.J. Gorte, “The effect of Ca, Sr, and Ba doping on the ionic conductivity and cathode performance of LaFeO₃”, *J. Electrochem. Soc.*, **155** [7] (2008) B660–B665.
 38. A.T. Nguyen, I.Ya. Mittova, O.V. Almjasheva, S.A. Kirillova, V.V. Gusarov, “Influence of the preparation condition on the size and morphology of nanocrystalline lanthanum orthoferrite”, *Glass Phys. Chem.*, **34** [6] (2008) 756–761.
 39. A.T. Nguyen, I.Ya. Mittova, O.V. Almjasheva, “Influence of the synthesis condition on the particle size and morphology of yttrium orthoferrite obtained”, *Russ. J. Appl. Chem.*, **82** [11] (2009) 1915–1918.
 40. V.V. Kharton, A.V. Kovalevsky, M.V. Patrakeev, E.V. Tsipis, A.P. Viskup, V.A. Kolotygin, A.A. Yaremchenko, A.L. Shaula, E.A. Kiselev, J.C. Waerenborg, “Oxygen nonstoichiometry, mixed conductivity, and Mössbauer spectra of Ln_{0.5}A_{0.5}FeO_{3-δ} (Ln = La–Sm, A = Sr, Ba): Effect of cation size”, *Chem. Mater.*, **20** [20] (2008) 6457–6467.
 41. H.W. Brinks, H. Fjellvag, A. Kjekshus, B.C. Hauback, “Structure and magnetism of Pr_{1-x}Sr_xFeO_{3-δ}”, *J. Solid State Chem.*, **150** [2] (2000) 233–249.
 42. B.D. Cullity, C.D. Graham, *Introduction to Magnetic Materials*, 2nd Ed., John Wiley & Sons Inc. Publication, Canada, 2009.
 43. T. Moriya, “New mechanism of anisotropic superexchange interaction”, *Phys. Rev. Lett.*, **4** (1960) 228–230.
 44. A.T. Nguyen, N.T.V. Pham, T.H. Le, H.D. Chau, V.O. Mittova, T.T.L. Nguyen, A.D. Dinh, P.V. Nhan Hao, I.Ya. Mittova, “Crystal structure and magnetic properties of LaFe_{1-x}Ni_xO₃ nanomaterials prepared via a simple coprecipitation method”, *Ceram. Int.*, **45** [17] (2019) 21768–21772.
 45. M.B. Bellakki, V. Manivannan, “Synthesis, and study of magnetic properties of Bi_{1-x}Cd_xFeO₃”, *J. Mater. Sci.*, **45** [4] (2010) 1137–1142.